

ASC Report No. 37/2012

# **Combining micromagnetism and magnetostatic Maxwell equations for multiscale magnetic simulations**

F. Bruckner, C. Vogler, B. Bergmair, T. Huber, M. Fuger,  
D. Suess, M. Feischl, T. Führer, M. Page, D. Praetorius

Institute for Analysis and Scientific Computing  
Vienna University of Technology — TU Wien  
[www.asc.tuwien.ac.at](http://www.asc.tuwien.ac.at) ISBN 978-3-902627-05-6

## Most recent ASC Reports

- 36/2012 *M. Bukal, E. Emmrich, and A. Jüngel*  
Entropy-stable and entropy-dissipative approximations of a fourth-order quantum diffusion equation
- 35/2012 *W. Auzinger and M. Tutz*  
A review of stability and error theory for collocation methods applied to linear boundary value problems
- 34/2012 *F. Bruckner, M. Feischl, T. Führer, P. Goldenits, M. Page, D. Praetorius and D. Süß*  
Multiscale Modeling in Micromagnetics: Well-Posedness and Numerical Integration
- 33/2012 *H. Winkler, H. Woracek*  
Symmetry in de Branges almost Pontryagin spaces
- 32/2012 *H. Hofstätter, O. Koch, M. Thalhammer*  
Convergence of split-step generalized-Laguerre-Fourier-Hermite methods for Gross-Pitaevskii equations with rotation term
- 31/2012 *S. Esterhazy and J.M. Melenk*  
An analysis of discretizations of the Helmholtz equation in  $L^2$  and in negative norms (extended version)
- 30/2012 *H. Hofstätter, O. Koch*  
An Approximate Eigensolver for Self-Consistent Field Calculations
- 29/2012 *A. Baranov, H. Woracek*  
De Branges' theorem on approximation problems of Bernstein type
- 28/2012 *B. Schörkhuber, T. Meurer, and A. Jüngel*  
Flatness of semilinear parabolic PDEs - A generalized Cauchy-Kowalevski approach
- 27/2012 *R. Donninger and B. Schörkhuber*  
Stable blow up dynamics for energy supercritical wave equations

Institute for Analysis and Scientific Computing  
Vienna University of Technology  
Wiedner Hauptstraße 8–10  
1040 Wien, Austria

**E-Mail:** [admin@asc.tuwien.ac.at](mailto:admin@asc.tuwien.ac.at)  
**WWW:** <http://www.asc.tuwien.ac.at>  
**FAX:** +43-1-58801-10196

ISBN 978-3-902627-05-6

© Alle Rechte vorbehalten. Nachdruck nur mit Genehmigung des Autors.



# Combining Micromagnetism and Magnetostatic Maxwell Equations for Multiscale Magnetic Simulations

Florian Bruckner<sup>a,\*</sup>, Christoph Vogler<sup>a</sup>, Bernhard Bergmair<sup>a</sup>, Thomas Huber<sup>a</sup>, Markus Fuger<sup>a</sup>, Dieter Suess<sup>a</sup>, Michael Feischl<sup>b</sup>, Thomas Fuehrer<sup>b</sup>, Marcus Page<sup>b</sup>, Dirk Praetorius<sup>b</sup>

<sup>a</sup>*Vienna University of Technology, Inst. Solid State Physics, Austria*

<sup>b</sup>*Vienna University of Technology, Inst. Analysis and Scientific Computing, Austria*

---

## Abstract

Magnetostatic Maxwell equations and the Landau-Lifshitz-Gilbert (LLG) equation are combined to a multiscale method, which allows to extend the problemsize of traditional micromagnetic simulations. By means of magnetostatic Maxwell equations macroscopic regions can be handled in an averaged and stationary sense, whereas the LLG allows to accurately describe domain formation as well as magnetization dynamics in some microscopic subregions. The two regions are coupled by means of their strayfield and the combined system is solved by an optimized timeintegration scheme.

*Keywords:* LLG, Micromagnetism, magnetostatic Maxwell equations, multiscale, timeintegration

---

## 1. Introduction

Micromagnetic simulations are utilized in a wide range of applications ranging from magnetic storage devices, permanent magnets to spintronic devices. With increasing complexity of the devices more properties have to be included in the simulations in order to predict the functional behavior of the structures accurately. State of the art micromagnetic simulations can handle systems with several millions of unknowns. In order to tackle these large scale problems both (i) new hardware architectures [1, 2] as well as (ii) advanced numerical methods are required.

Newly developed numerical methods focus on speeding up the two most time consuming parts in micromagnetic simulations, which are the calculation of the strayfield and the time integration of the LLG equation. Advanced time integrations schemes can be found in Ref. [3–8]. For the calculation of the strayfield advanced FFT algorithms [9, 10], fast multipole methods [11, 12], nonuniform grid methods [13], FEM/BEM coupling approaches including compression of the boundary matrix [14–16], and tensor grid methods [17, 18] have been developed.

Aside from new algorithms solving the micromagnetic model efficiently for systems with many degrees of freedom, it is often possible to choose a simplified physical model to describe at least some parts of the total problem. By this way the number of degrees of freedom can be reduced dramatically without losing accuracy in regions where it is desired. Within this paper we will utilize the fact that models described by the LLG equation require very fine grained discretization which can lead to impractically large system sizes. We propose using the LLG equation to describe only those regions of the problem where detailed information about the domain structure such as domain walls and vortex structures are required. For the rest of the model a macroscopic description via magnetostatic Maxwell equations is chosen. Since it does not resolve the detailed domainstructure it allows to use much coarser discretization.

The structure of the paper is as follows. Section 2 summarizes the methods that are used to individually solve the LLG equations or magnetostatic Maxwell equations respectively. How the two systems can be coupled in an efficient way is described in section 3. Finally in section 4 the multiscale algorithm is applied to the simulation of a magnetic giant magnetoresistance (GMR) readhead and numerical results and benchmarks are presented.

---

\*Corresponding author

*Email address:* `florian.bruckner@tuwien.ac.at` (Florian Bruckner)

## 2. Fundamentals

For the coupling of micromagnetism and magnetostatic Maxwell equations the full model is divided into two separated regions (see Fig. 1). The LLG equation is used to describe the first region, where domain structure, short range interactions or the magnetization dynamics of the magnetic parts is of great interest. The second region is described by magnetostatic Maxwell equations, which describe the magnetic state in a spacially averaged sense and without dynamics. Since both models contain the external field as a source term, coupling via the strayfield can be achieved in a straight forward way. The strayfield created from the LLG model can be considered as an external field of the Maxwell model and vice versa. In the following subsections it is shown how the two sub-problems are solved individually.

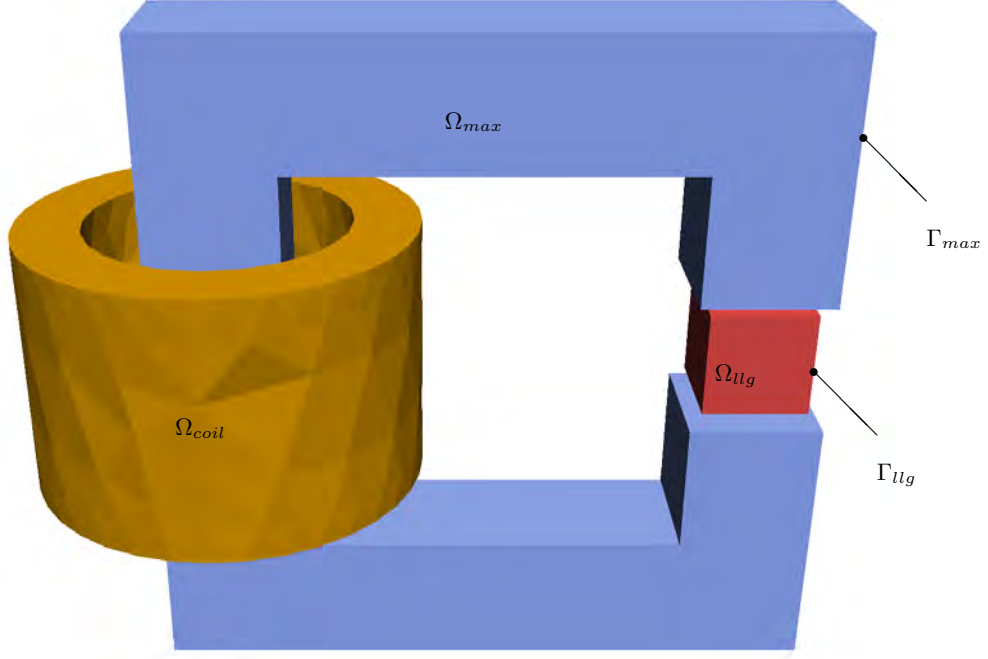


Figure 1: Example geometry which demonstrates model separation into LLG region  $\Omega_{llg}$  and Maxwell region  $\Omega_{max}$  (and in this case in an electric coil region  $\Omega_{coil}$ ). The boundaries of the regions are called  $\Gamma_{llg}$  and  $\Gamma_{max}$  respectively.

### 2.1. LLG

The LLG equation describes how magnetic polarizations  $\mathbf{J}$  (with a fixed modulus  $J_s$ ) evolve in an effective field  $\mathbf{H}_{\text{eff}}$ . It consists of a precessional term as well as a phenomenological damping term:

$$\frac{\partial \mathbf{J}}{\partial t} = -\frac{|\gamma|}{1+\alpha^2} \mathbf{J} \times \mathbf{H}_{\text{eff}} - \frac{\alpha}{1+\alpha^2} \frac{|\gamma|}{J_s} \mathbf{J} \times \mathbf{J} \times \mathbf{H}_{\text{eff}} \quad (1)$$

where  $\alpha$  is the Gilbert damping constant,  $J_s$  is the saturation polarization and  $|\gamma| = 2.210175 \cdot 10^5 \text{ m/As}$  is the gyromagnetic ratio. The effective field can be split into four contributions as follows:

$$\begin{aligned} \mathbf{H}_{\text{eff}} &= \mathbf{H}_{\text{ex}} + \mathbf{H}_{\text{ani}} + \mathbf{H}_{\text{demag}} + \mathbf{H}_{\text{ext}} = \\ &= \frac{2A}{J_s^2} \Delta \mathbf{J} + \frac{2}{J_s^2} K_1 (\mathbf{J} \cdot \mathbf{a}) \mathbf{a} + \mathbf{H}_{\text{demag}} + \mathbf{H}_{\text{ext}} \end{aligned} \quad (2)$$

$\mathbf{H}_{\text{ex}}$  describes the short-range exchange interaction parametrized by the exchange constant  $A$ .  $\mathbf{H}_{\text{ani}}$  stands for the magneto-crystalline anisotropy field with the linear anisotropy constant  $K_1$  and the easy axis  $\mathbf{a}$ . The magnetic strayfield  $\mathbf{H}_{\text{demag}}$  describes the long-range interaction between the magnetic moments within the magnetic media.  $\mathbf{H}_{\text{ext}}$  is the applied field, which can for example be created by an electric coil, or as described later on by a Maxwell model. In addition to the mentioned fields several other contributions are possible, like stochastic fields for thermal calculations, or a magneto-elastic term that describes how the magnetic fields influence the mechanical properties of the magnetic part.

To calculate the strayfield created by a given magnetization distribution, which is needed for  $\mathbf{H}_{\text{demag}}$  and also for the interaction between LLG and Maxwell parts, the Fredkin-Koehler-Method [14] is used. Basically the following potential equations are solved for given  $\mathbf{J}$

$$\nabla^2 u_{llg} = \nabla \cdot \mathbf{J} \quad \text{in } \Omega_{llg} \quad (3a)$$

$$\nabla^2 u_{llg} = 0 \quad \text{in } \mathbb{R}^3 \setminus \Omega_{llg} \quad (3b)$$

$$[u_{llg}] = 0 \quad \text{on } \Gamma_{llg} \quad (3c)$$

$$\left[ \frac{\partial u_{llg}}{\partial \mathbf{n}} \right] = \mathbf{n} \cdot \mathbf{J} \quad \text{on } \Gamma_{llg} \quad (3d)$$

where  $[x]$  means the jump of value  $x$  at the surface of the LLG region. The strayfield finally reads as  $\mathbf{H}_{\text{demag}} = -\mu_0^{-1} \nabla u_{llg}$ .

A detailed description of how the LLG equation is actually solved as well as a proper preconditioning method to speed up calculations of large problems can be found in [3].

### 2.2. Magnetostatic Maxwell Equations

Magnetostatic Maxwell equations are used to describe stationary phenomena averaged over a sufficiently large area. As a result of this description the modulus of the magnetic polarizations is not constant, but depends on the local magnetic field. Since the material behavior is only described in average, its description leads to a more complicated (in general nonlinear) material law. The advantage of this approach is that it allows to discretize the geometry much coarser, because domains need not be resolved, and that it allows to ignore the possibly disturbing dynamics of the macroscopic parts.

The fundamental equations that have to be solved within the Maxwell region are:

$$\text{rot } \mathbf{H} = \mathbf{j} \quad \text{div } \mathbf{B} = 0 \quad (4a)$$

$$\mathbf{B} = \mu_0(\mathbf{H} + \mathbf{M}) = \mu_0 \mu \mathbf{H} \quad (4b)$$

where the current density  $\mathbf{j}$  is the source of the magnetic field strength  $\mathbf{H}$  which is related to the magnetic flux density  $\mathbf{B}$  via the relative permeability  $\mu$  (which may depend on the location and in the nonlinear case also on the local field strength) times the vacuum permeability  $\mu_0 = 4\pi 10^{-7} \text{Vs/Am}$ . In contrast to the strayfield calculation of the LLG model the magnetization  $\mathbf{M}$  is not known a priori since it depends on the local magnetic field strength.

Introduction of a reduced scalar potential  $u_{max}$  by setting  $\mathbf{H} = \mathbf{H}_{\text{ext}} - \nabla u_{max}$  directly solves the homogeneous Maxwell equation and combined with proper jump condition at the boundary of the magnetic parts it leads to:

$$\nabla \cdot (\mu \nabla u_{max}) = \nabla \cdot (\mu^+ \mathbf{H}_{\text{ext}}) \quad \text{in } \Omega_{max} \quad (5a)$$

$$\nabla^2 u_{max} = 0 \quad \text{in } \mathbb{R}^3 \setminus \Omega_{max} \quad (5b)$$

$$[u_{max}] = 0 \quad \text{on } \Gamma_{max} \quad (5c)$$

$$\left[ \mu \frac{\partial u_{max}}{\partial \mathbf{n}} \right] = [\mu] \mathbf{n} \cdot \mathbf{H}_{\text{ext}} \quad \text{on } \Gamma_{max} \quad (5d)$$

where  $[x]$  means the jump of value  $x$  at the surface of the Maxwell region.

A detailed description of the methods used to solve the magnetostatic Maxwell equations can be found in [19].

### 2.3. Discretization

The inhomogeneities within the LLG- as well as within the Maxwell-domain are discretized by means of finite elements. Within the LLG domain the element size is constrained by the exchange length of the used material. Typical values are in the range of  $10 \text{nm}$ . Choosing larger elements would lead to unphysically large domain wall widths. For the Maxwell region such constraint does not exist, which allows to use much bigger elements in some regions.

In both cases FEM-BEM coupling methods are applied to handle the open-boundary problem. In addition to the fact that these methods are well suited for the solution of the individual problems they also simplify the coupling of the two methods because each methods can be solved on its individual mesh without the need for a global mesh. The strayfield produced by each model which is needed to handle interactions can be calculated at any point by means of the boundary element formulas.

### 3. Coupling Method

In order to solve the coupled problem one needs to deal with ordinary differential equations (ODE), which arise from the discretization of the LLG equations, as well as with algebraic equations arising from Maxwell's equations. Discretization of this system of Differential-Algebraic-Equations (DAE) using integration methods for ODEs can lead to numerical instabilities or to a drift error in the algebraic equations [20]. Therefore differential and algebraic equations are kept separate and a sequential method is used to combine both problems.

For time discretization the backward differential formula (BDF) is applied to the ODE system and is in turn solved by means of an Inexact Newton method (we therefore used the open source differential equation solver CVODE [21]). Inside of the time integration algorithm Eqn. (1) needs to be evaluated several times and at this step the interaction with the Maxwell equations (5) is considered. Every time the function is evaluated, first the strayfield created by the actual magnetization within the LLG part is calculated. With this strayfield contribution the Maxwell system is solved by means of another Inexact Newton method. After the Maxwell system is solved the back-interaction on the LLG model can be calculated and allows to finally evaluate the LLG system. This procedure leads to a fully implicit scheme to solve the coupled equation.

#### 3.1. Optimization

Solving the Maxwell problem within every function evaluation of the LLG time-integration can be very time-consuming for considerably large Maxwell models. Fortunately the simulation can be speeded up by using the recent theoretical prediction [22] that for stability of the time-integration only the exchange interaction term needs to be handled implicitly. All other terms, including the interaction with the Maxwell model, can be handled explicitly, which means that we simply use the interaction field of the last timestep to evaluate all function values needed at the next timestep. Thus we only need to solve the Maxwell problem once for every non-linear step of the time-integration.

## 4. Results

### 4.1. Problem Description

In this section the developed algorithm is applied to calculate the transfer curve [23] of a magnetic readhead setup (see Fig. 2). For the transfer curve a homogeneous external field perpendicular to the media is applied to the whole setup and the stationary output of the readhead is plotted as a function of the field strength. The media is not considered in this simulation.

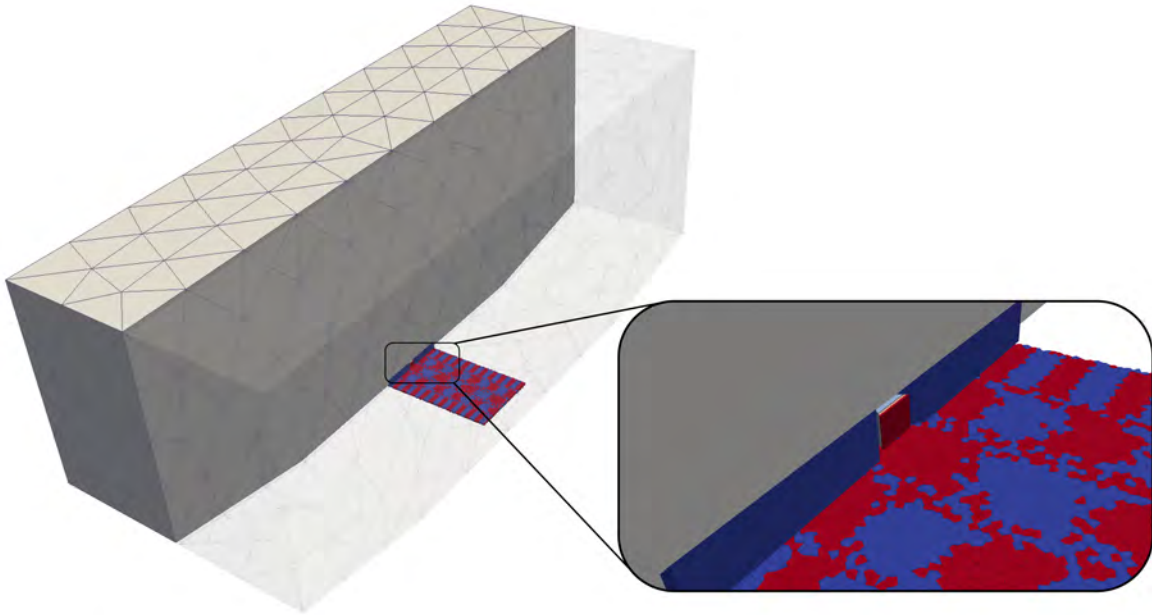


Figure 2: The example setup consists of a GMR sensor element in between two macroscopic shields. Beyond the GMR sensor a magnetic storage media is indicated (it will not be considered for the calculation of the transfer curves).

The (GMR) reader element consists of microscopic layers which can be well described by the LLG. On the other hand the setup consists of macroscopic shields which have the purpose to reduce the influence of the strayfield from neighboring bits on the output signal of the current bit. Since these shields are separated from the sensor element and its domain structure is not of interest, it is possible to describe them using magnetostatic Maxwell equations. Additionally for the transfer curve stationary states for different values of the external fields are needed, which means that the dynamic of the shields can be safely ignored in this case. Therefore the usage of the multiscale method allows to reduce the simulation time significantly.

The detailed structure of the giant magnetoresistance sensor is shown in Fig. 3.

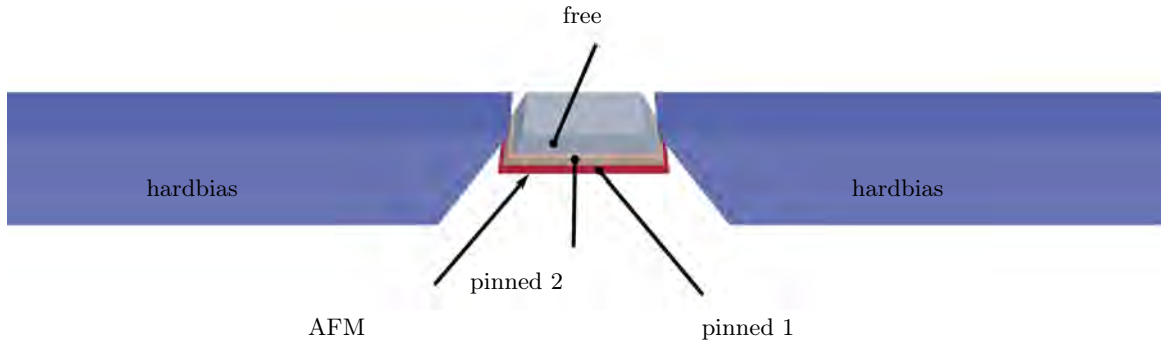


Figure 3: The GMR reader element for our testcase consists of two pinned layers which are antiferromagnetically coupled via a thin Ruthenium layer between them. Their magnetization is pinned by a granular antiferromagnetic layer below the bottom layer. The freelay is located above the pinned layers and its initial magnetization is forced orthogonal to the magnetization of the pinned layer by means of two hardbias magnets. The output signal of the sensor element is proportional to the cosine of angle  $\phi$  between the magnetization within the pinned- and the free-layer.

Due to the GMR effect the resistance of the freelay changes depending on the cosine of angle  $\phi$  between the magnetization within free- and pinned layer. The transfer curve thus shows  $\cos(\phi)$  for various external field strengths.

#### 4.2. Simulation Results

In order to demonstrate the strengths of the presented algorithm we calculate transfer curves for different grid sizes of the magnetic shields (see Fig. 4). For the material of the Maxwell part we use a linear material law with permeability  $\mu = 1000$  up to the saturation polarization  $J_s$ , which is the same as in the LLG-only case. Results are compared with LLG-only simulations of the same model. Since dynamic effects still seem to play an important role in the LLG-only simulation when using the same external field rise time as for the multiscale algorithm (see Fig. 5), another simulation was done using the LLG-only model with a much slower rise time (see Fig. 6). The increase of the rise time leads to significant reduction of the dynamic artefacts within the simulated transfer curves. Finally a comparison of the different algorithms for proper grid sizes as well as field sweep rates (see Fig. 7) shows that the results are in good agreement with each other, provided that one uses a saturated material law within the Maxwell part.

A comparison of the performance of the multiscale algorithm with and without optimization, as well as with LLG-only methods is presented in Tab. 1.

## 5. Conclusion

A multiscale algorithm was presented which combines the capabilities of LLG- as well as Maxwell- equation solvers and allows to handle much larger problem sizes. Coupling the LLG to the Maxwell part could be optimized by handling the corresponding terms explicitly within the time integration scheme. Finally the optimized algorithm was validated by means of a transfer curve simulation of a magnetic readhead. The results of the multiscale algorithm match very well with those of the LLG-only simulation, but it allows to significantly reduce the shield gridsize and to increase the field sweep rates.

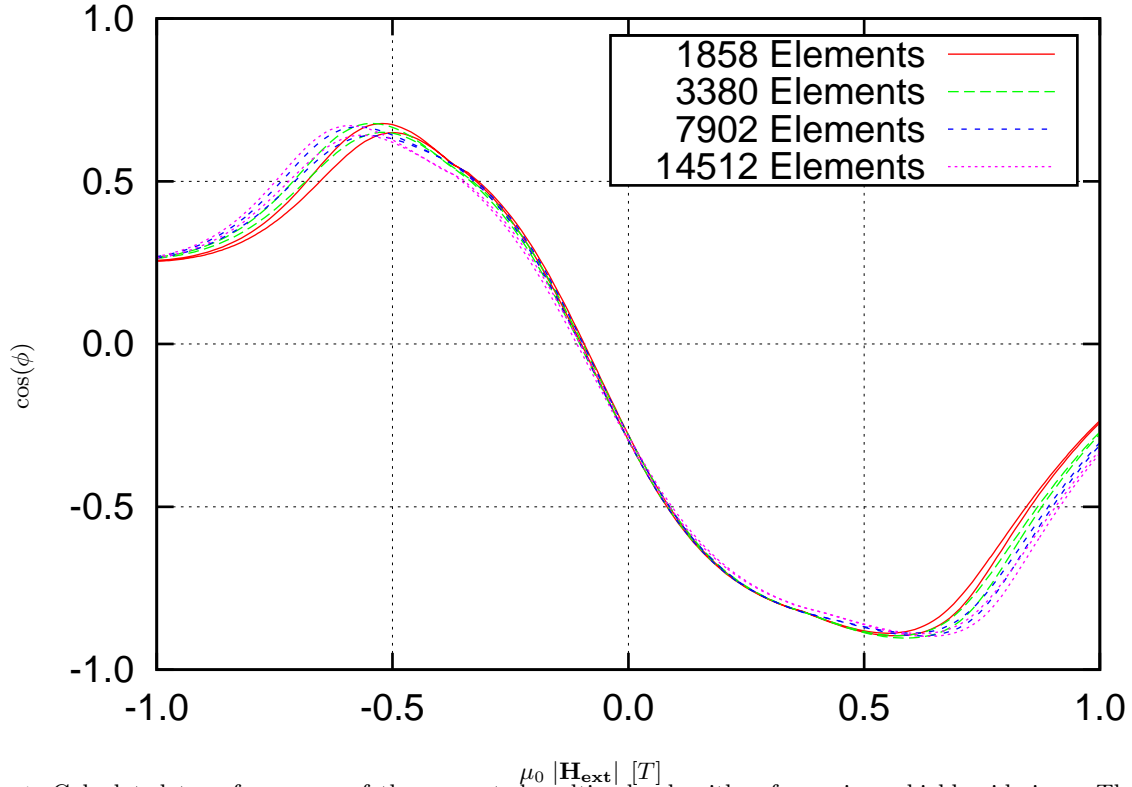


Figure 4: Calculated transfer curves of the presented multiscale algorithm for various shield grid sizes. The angle  $\phi$  between the magnetizations within pinned- and free-layer is plotted as a function of the external field  $\mathbf{H}_{\text{ext}}$ . The algorithm starts to produce convergent results at around 1000 elements and due to the use of magnetostatic equations it shows no dynamic artifacts.

	LLG*	LLG (conv.)	Multiscale	Multiscale (optimized)
$t_{\text{sim}}$ [ns]	70	1000	70	70
$N_{\text{shield}}$	3380	39032	3380	3380
$N_{\text{max}}$	-	-	22274	6038
$N_{\text{llg}}$	69584	173227	22274	22203
$t_{\text{run}}$ [s]	1084	173184	11857	8107

Table 1: Algorithm performance for the transfer curve calculation.  $t_{\text{run}}$  is the overall runtime of the simulation. The simulation period  $t_{\text{sim}}$  as well as the shield grid size  $N_{\text{shield}}$  are chosen in a way that the algorithm produces convergent results (LLG\* shows non-converged results and is listed only to give a reference time scale).  $N_{\text{max}}$  and  $N_{\text{llg}}$  are the number of times the Maxwell- or the LLG-part is evaluated, respectively.

## Acknowledgment

The authors would like to thank the WWTF Project MA09-029 and FWF Project SFB-ViCoM F4112-N13 for the financial support.

- [1] A. Vansteenkiste, B. Van de Wiele, MuMax: a new high-performance micromagnetic simulation tool, arXiv:1102.3069.
- [2] S. Li, B. Livshitz, V. Lomakin, Graphics processing unit accelerated  $O(N)$  micromagnetic solver, IEEE Trans. Magn. 46 (2010) 2373–2375.
- [3] D. Suess, V. Tsiantos, T. Schrefl, J. Fidler, W. Scholz, H. Forster, R. Dittrich, J. Miles, Time resolved micromagnetics using a preconditioned time integration method, Journal of Magnetism and Magnetic Materials 248 (2002) 298–311.
- [4] M. d’Aquino, C. Serpico, G. Miano, Geometrical integration of Landau-Lifshitz-Gilbert equation based on the mid-point rule, J. Comput. Phys. 209 (2005) 730–753.



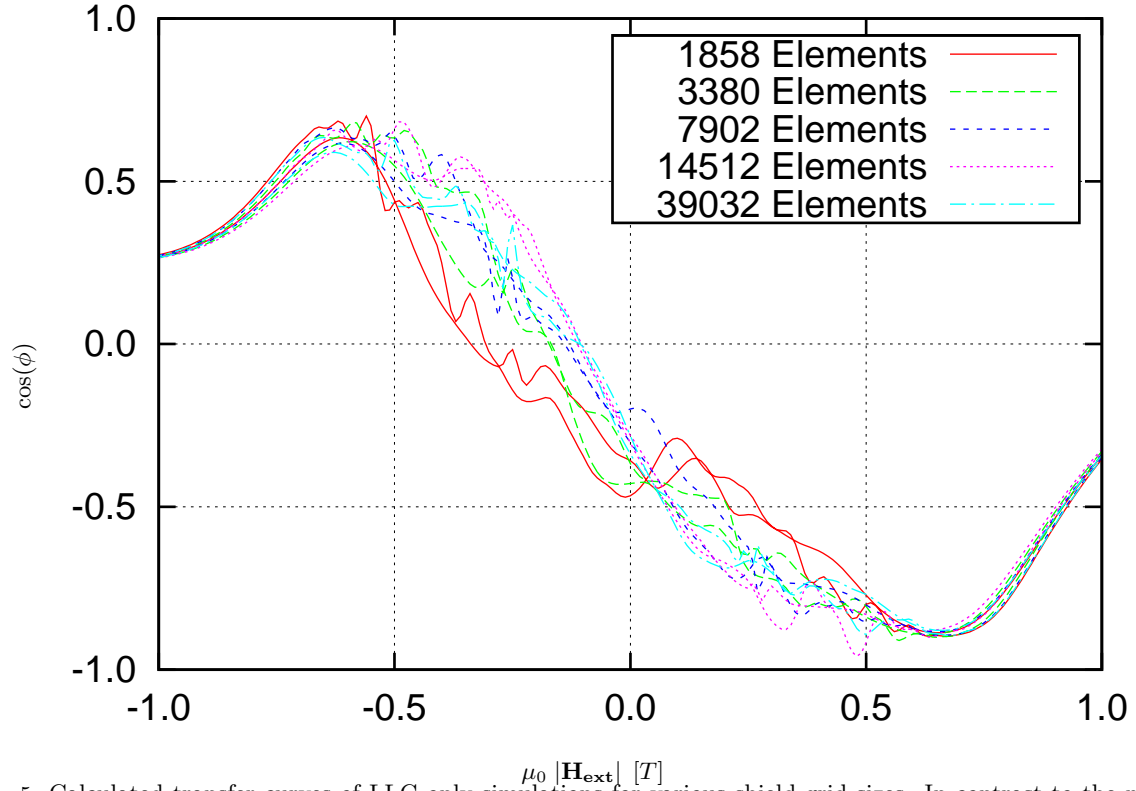


Figure 5: Calculated transfer curves of LLG-only simulations for various shield grid sizes. In contrast to the multiscale algorithm it shows some significant deviations up to at least 50 000 elements. Additionally there occur some artifacts due to the large timeconstant of the magnetization dynamic within the macroscopic shields. The field sweep rate is chosen too high to reach the equilibrium state and therefore leads to some fluctuations within the transfer curves.

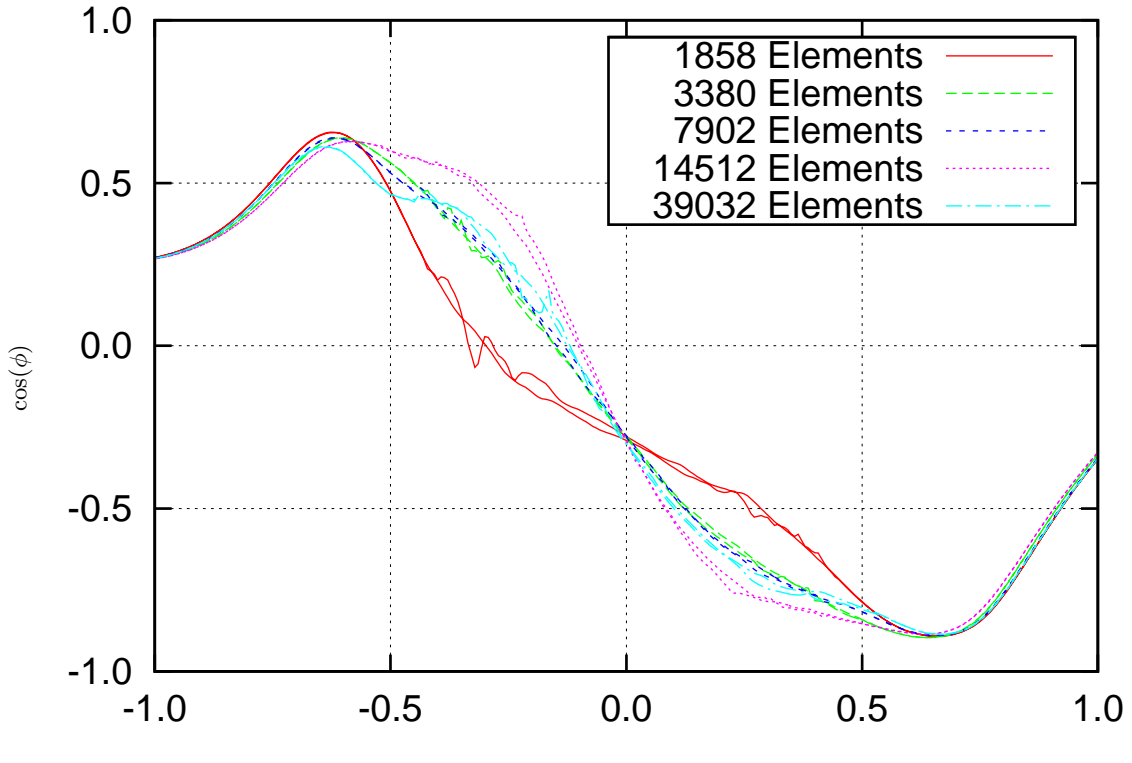


Figure 6: Calculated transfer curves of LLG-only simulations using a field sweep rate reduced by a factor 5. The fluctuations are reduced, but there are still significant differences due to the coarse shield discretization.

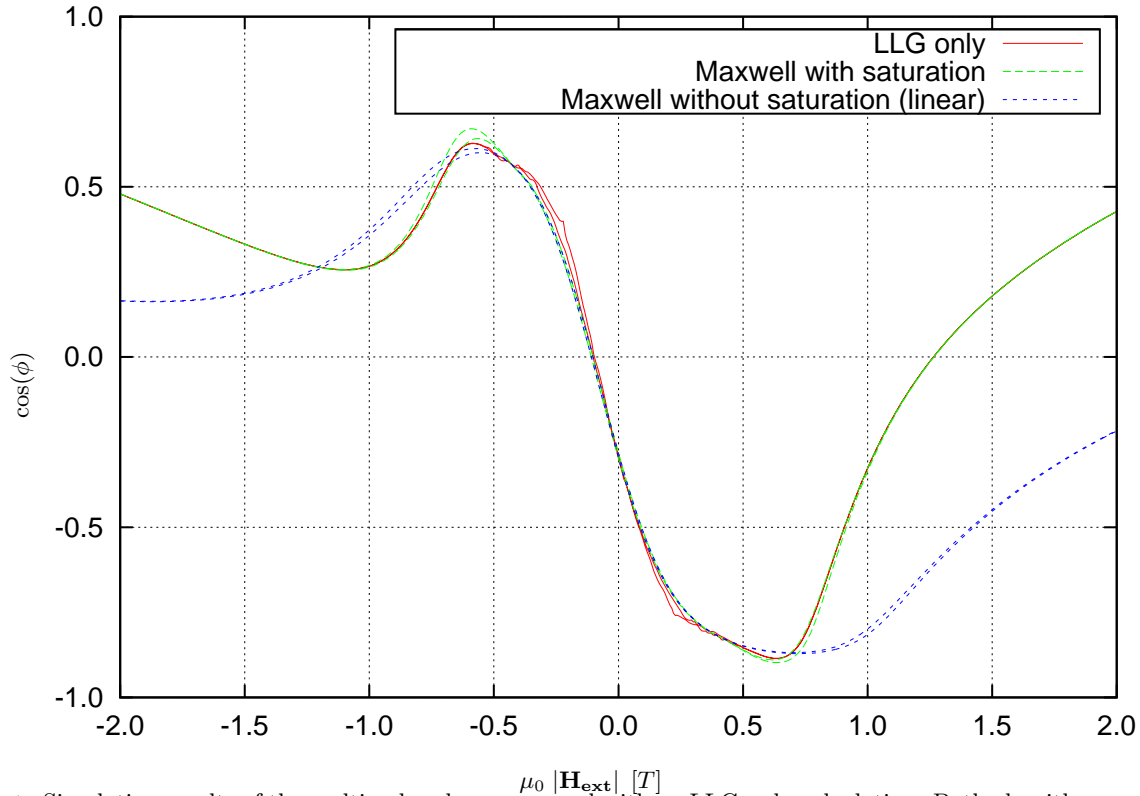


Figure 7: Simulation results of the multiscale solver compared with an LLG-only calculation. Both algorithms are applied to the same model with 14512 elements. A permeability of  $10^3$  is used for the material of the shields within the Maxwell solver. In order to get matching results at high fields one needs to use a saturated material law.

- [5] M. Slodička, L. Bañas, A numerical scheme for a Maxwell-Landau-Lifshitz-Gilbert system, *Appl. Math. Comput.* 158 (2004) 79–99.
- [6] X. Wang, C. J. García-Cervera, W. E, A Gauss-Seidel projection method for micromagnetics simulations, *J. Comput. Phys.* 171 (2001) 357–372.
- [7] F. Alouges, E. Krittikis, J. Toussaint, A convergent finite element approximation for Landau-Lifschitz-Gilbert equation, *Physica B* 407 (2012) 1345–1349.
- [8] P. Goldenits, G. Hrkac, D. Praetorius, D. Suess, An effective integrator for the Landau-Lifshitz-Gilbert equation, in: *Proceedings of Mathmod 2012 Conference - to appear.*
- [9] C. Abert, G. Selke, B. Kruger, A. Drews, A fast Finite-Difference method for micromagnetics using the magnetic scalar potential, *IEEE Trans. Magn.* 48 (2012) 1105–1109.
- [10] Y. Kanai, M. Saiki, K. Hirasawa, T. Tsukamoto, K. Yoshida, Landau-Lifshitz-Gilbert micromagnetic analysis of Single-Pole-Type write head for perpendicular magnetic recording using Full-FFT program on PC cluster system, *IEEE Trans. Magn.* 44 (2008) 1602–1605.
- [11] R. K. Beatson, L. Greengard, A short course on fast multipole methods, *Wavelets, multilevel methods and elliptic PDEs* (1997) 1–37.
- [12] J. Blue, M. Scheinfein, Using multipoles decreases computation time for magnetostatic self-energy, *IEEE Trans. Magn.* 27 (1991) 4778–4780.
- [13] B. Livshitz, A. Boag, H. N. Bertram, V. Lomakin, Nonuniform grid algorithm for fast calculation of magnetostatic interactions in micromagnetics, *J. Appl. Phys.* 105.
- [14] D. Fredkin, T. Koehler, Hybrid method for computing demagnetizing fields, *IEEE Trans. Magn.* 26 (1990) 415–417.
- [15] A. Knittel, M. Franchin, G. Bordignon, T. Fischbacher, S. Bending, H. Fangohr, Compression of boundary element matrix in micromagnetic simulations, *J. Appl. Phys.* 105.

- [16] N. Popović, D. Praetorius, Applications of H-Matrix techniques in micromagnetics, *Computing* 74 (2005) 177–204.
- [17] L. Exl, W. Auzinger, S. Bance, M. Gusenbauer, F. Reichel, T. Schrefl, Fast stray field computation on tensor grids, *J. Comput. Phys.* 231 (2012) 2840–2850.
- [18] A. Goncharov, G. Hrkac, J. Dean, T. Schrefl, Kronecker product approximation of demagnetizing tensors for micromagnetics, *J. Comput. Phys.* 229 (2010) 2544–2549.
- [19] F. Bruckner, C. Vogler, M. Feischl, D. Praetorius, B. Bergmair, T. Huber, M. Fuger, D. Suess, 3D FEM-BEM-coupling method to solve magnetostatic maxwell equations, *Journal of Magnetism and Magnetic Materials* 324 (2012) 1862–1866.
- [20] L. R. Petzold, Differential/algebraic equations are not ODEs, *SIAM J. Sci. Stat. Comput* 3 (1982) 367–384.
- [21] A. Hindmarsh, P. Brown, K. Grant, S. Lee, R. Serban, D. Shumaker, C. Woodward, SUNDIALS: suite of nonlinear and differential/algebraic equation solvers, *ACM Trans. Math. Softw.* 31 (2005) 363–396.
- [22] F. Bruckner, M. Feischl, T. Führer, M. Page, D. Praetorius, D. Suess, Multiscale modeling in micromagnetics: well-posedness and numerical integration, work in progress 2012.
- [23] S. She, D. Wei, Y. Zheng, B. Qu, T. Ren, X. Liu, F. Wei, Micromagnetic simulation of transfer curve in giant-magnetoresistive head, *Chinese Phys. Lett.* 26.